Molecular Dynamics of a Cytochrome c–Cytochrome b_5 Electron Transfer Complex

J. J. WENDOLOSKI, JAMES B. MATTHEW, P. C. WEBER, F. R. SALEMME

Cytochrome c and cytochrome b_5 form an electrostatically associated electron transfer complex. Computer models of this and related complexes that were generated by docking the x-ray structures of the individual proteins have provided insight into the specificity and mechanism of electron transfer reactions. Previous static modeling studies were extended by molecular dynamics simulations of a cytochrome c–cytochrome b_5 intermolecular complex. The simulations indicate that electrostatic interactions at the molecular interface result in a flexible association complex that samples alternative interheme geometries and molecular conformations. Many of these transient geometries appear to be more favorable for electron transfer than those formed in the initial model complex. Of particular interest is a conformational change that occurred in phenylalanine 82 of cytochrome c that allowed the phenyl side chain to bridge the two cytochrome heme groups.

ELECTRON TRANSFER REACTIONS between proteins control the flow and conservation of energy in biological organisms. Many questions remain about the geometrical and physical requirements for efficient electron transfer, particularly between proteins forming transient complexes that are difficult to examine directly by x-ray crystallography. Nevertheless, computer models of molecular complexes that are obtained by docking the x-ray structures of the reaction partners have provided useful insight into the structural origins of molecular recognition and reactivity. One extensively studied system is the reversible reaction complex formed between mitochondrial cytochrome c and microsomal cytochrome b_5. Structure-function studies of this complex were motivated by the x-ray structure determinations of mitochondrial cytochrome c (*1*) and the related bacterial cytochrome c_2 (*2*). These structures showed that the heme prosthetic groups were partially exposed at the molecular surface and that both proteins shared a structurally analogous ring of positively charged lysine residues about the perimeters of their heme crevices (*3*), which suggested that the surface electrostatic interactions provided by the lysine "necklace" could facilitate oriented, two-dimensional diffusion on the biological membrane and allow the formation of transient, oriented interactions with membrane-bound oxidoreductases. Since surface diffusion would allow cytochrome c to form alternative interactions with membrane-bound oxidoreductases, both oxidation and reduction of the cytochrome c heme could occur via a common pathway at the exposed heme edge. Electron transfer by a classical outer-sphere mechanism might then occur through alternative van der Waals overlap of the porphyrin π orbital system of cytochrome c with the heme groups of the cognate oxidoreductases (*3, 4*).

Cytochrome b_5 reacts with cytochrome c at physiological rates (*5*). The x-ray structure of cytochrome b_5 (*6*) allowed the first computer modeling of a complex to test whether van der Waals contact could occur between the hemes of cytochrome c and cytochrome b_5 (*7*). Because of steric interference from groups at the complex interface, the closest approach between π-bonded porphyrin atoms was greater than 8 Å, a distance similar to theoretical estimates for electron transfer by a short-range tunneling mechanism (*8*). The model complex was otherwise characterized by good surface complementarity, nearly coplanar heme group orientation, and several charge-pair interactions formed between the ϵ-amino groups of evolutionarily conserved lysine residues on cytochrome c and the carboxylic acid groups on cytochrome b_5 (*7*).

Subsequent chemical modification and spectroscopic experiments have verified numerous aspects of the cytochrome c–cytochrome b_5 model complex (*9*). The static modeling approach has been extended to electron transfer complexes formed between either cytochrome c or cytochrome b_5 and other electron transfer proteins (*10*). These studies have facilitated the prediction of molecular surfaces involved in complex formation as well as physical effects such as the reaction rate dependence on ionic strength (*11*). Nevertheless, the static modeling studies leave many unanswered questions concerning complex formation and electron transfer mechanism. Among these is the role of dynamic fluctuations in sampling complex geometries that may differ from those in the static model but may be important in facilitating electron transfer. Molecular dynamics simulations of the cytochrome c–cytochrome b_5 complex were performed to

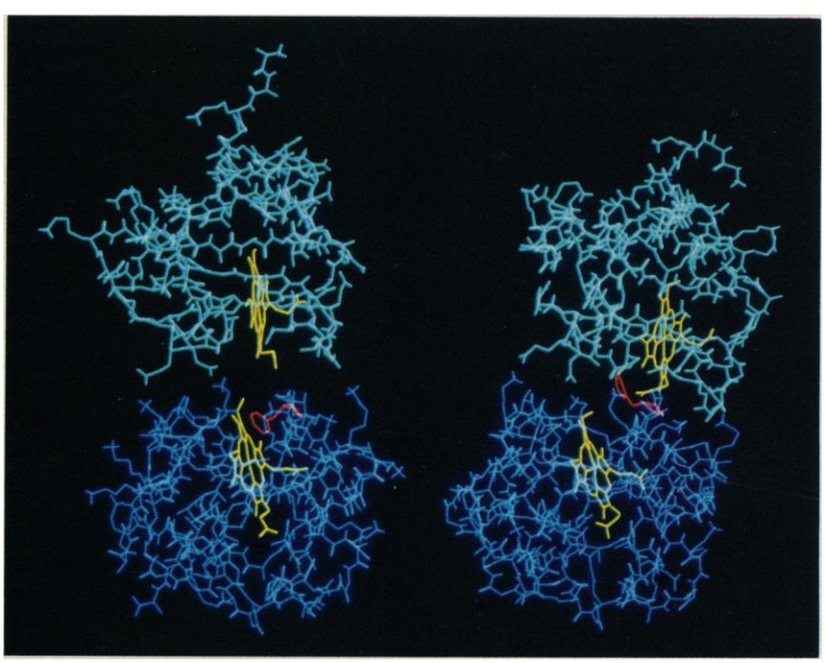

Fig. 1. Views of the cytochrome c–cytochrome b_5 electron transfer complex (left side) as initially energy minimized from the model produced by docking the crystal structures of the individual proteins, and (right side) after 46 psec of molecular dynamics simulation. In this 46-psec snapshot, the side chain of Phe^{82} lies coplanar with both heme groups of the cytochromes, an arrangement that may be favorable for electron transfer. In this figure and Fig. 3, only charged side chains, heme ligands, and Phe^{82} (red) of cytochrome c have been included for clarity. Cytochrome c is on the bottom of the complex in Figs. 1 and 3.

Central Research and Development Department, E. I. du Pont de Nemours and Company, Experimental Station 228/320A, Wilmington, DE 19898.

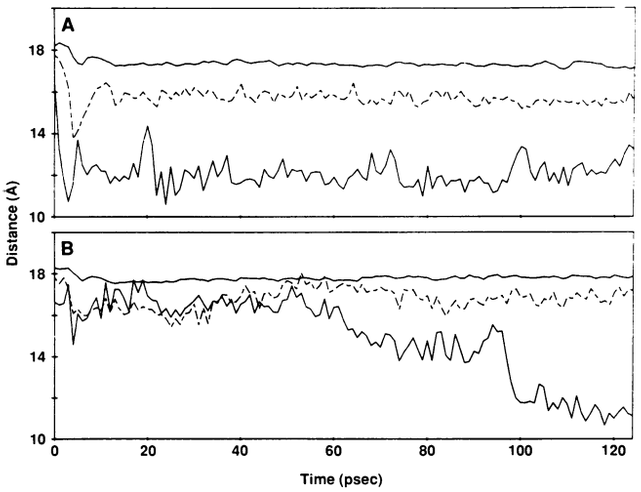

Fig. 2. Time evolution of representative geometrical interactions during (**A**) molecular dynamics simulation with a distance-dependent dielectric constant approximation, and (**B**) the simulation with the complex solvated with a 6 Å thick water shell. In each panel, the upper solid curve shows the complex radius of gyration, R_g, which is defined as $R_g = [(\Sigma m_i r_i^2)/(\Sigma m_i)]^{1/2}$, where m_i are the atomic masses and r_i are distances between each atom and the molecular center of mass. The dashed curve is the distance between the two heme iron centers, and the lower solid curve the distance between the center of the phenyl ring of Phe^{82} of cytochrome c and the heme iron of cytochrome b_5.

investigate dynamic factors that might influence electron transfer.

Figure 1 (left side) illustrates the cytochrome c–cytochrome b_5 complex (*7*) as reconstructed with interactive computer graphics manipulation of the crystal structures (*12*) and subjected to energy minimization (*13*); Fig. 1 (right side) shows the complex structure after 46 psec of molecular dynamics simulation with a potential function that incorporates a distance-dependent dielectric constant to approximate solvent screening effects on electrostatic interactions (*13*). Molecular dynamics alters the positions of the reaction partners in the complex, as is apparent from the shift in the relative heme group orientation shown in the two views of Fig. 1. In the 46-psec view, cytochrome b_5 has shifted from its initial position relative to cytochrome c in the static complex by 6.2 Å (Fig. 1, right). This is larger than the root-mean-square (rms) shifts that occurred in cytochrome c and b_5 individually (1.7 Å and 2.0 Å, respectively) and reflects substantial relative motion of the complex reaction partners.

Figure 2A illustrates the time evolution of two representative interactions in the complex; the distance between the heme iron centers of the two proteins, and the distance between the heme iron of cytochrome b_5 and the center of the ring of Phe^{82} of cytochrome c, a residue that is located at the complex interface. During the initial stage of the simulation there is an abrupt transient reduction in the inter-iron distance from 17.8 Å in the energy-minimized complex to 13.5 Å at 4.45 psec. The complex then rapidly relaxes so that the inter-iron distance fluctuates ±0.5 Å about an average distance of 15.7 Å for the remainder of the simulation. Both the initial compression and subsequent relaxation of the complex are also manifest in the time evolution of the complex radius of gyration.

Computer graphics examination of the dynamics trajectory also revealed local conformational changes that occurred during the simulation. The most interesting was a conformational change of Phe^{82} in cytochrome c. During the first few picoseconds of the simulation, Phe^{82} moved from its crystallographically observed location, where the side-chain phenyl group is packed near the cytochrome c heme, to a position where it bridges the porphyrin π orbital systems of both of the complex heme groups (Fig. 3). The side chain of Phe^{82} continues to sample many local orientations after the initial movement from the cytochrome c heme crevice. Some of these conformations, such as the 46-psec orientation shown in Fig. 1 (right side), could be particularly favorable for electron transfer. Most of the major changes in complex geometry occur abruptly during the first few picoseconds of the nonsolvated simulation, when opposing electrostatic interactions formed at the molecular interface impart large forces on the complex as it dynamically relaxes. Although electrostatic effects are potentially important in facilitating electron transfer, recent simulations of cytochrome c molecular dynamics have shown some differences in behavior that depend on the solvent or dielectric model used in the simulation (*14*).

To further evaluate the role of intermolecular electrostatic forces in the complex dynamics, a second 140-psec simulation (*15*) was performed on the complex that was explicitly solvated by a shell of water molecules 6 Å thick. Trajectory distance data for the solvated simulation are shown in Fig. 2B. Initial reductions in both complex radius of gyration and Fe-Fe distance are less pronounced in the solvated simulation than in the distance-dependent dielectric simulation. In the solvated simulation the inter-iron distance decreases from an initial value of 17.8 Å to an average of 16.7 Å for the

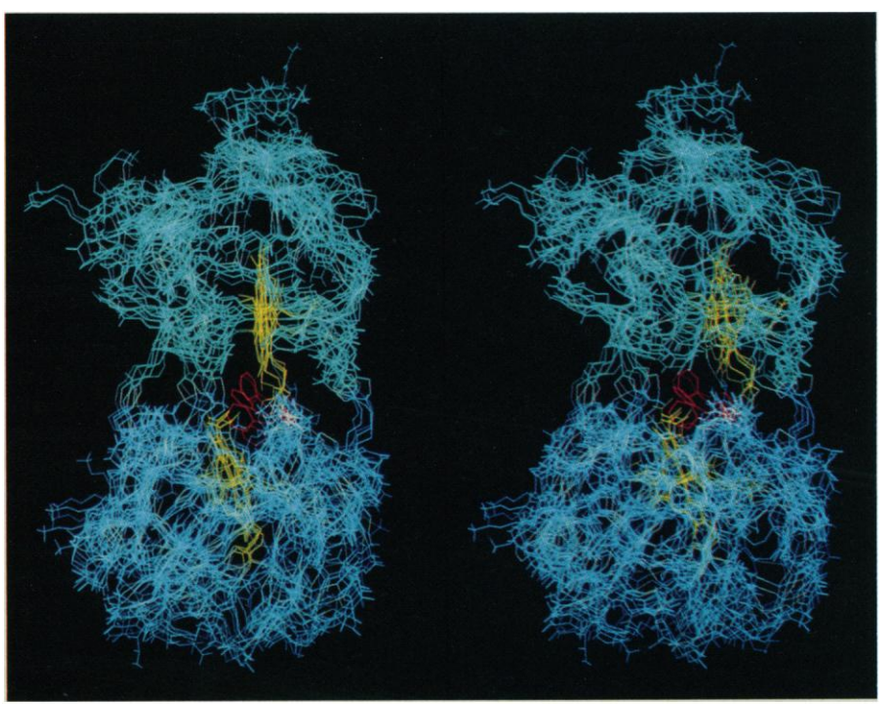

Fig. 3. Superimposed stereoscopic views of the complex at times t = 0, 1, 2, 3, 4, and 5 psec of the molecular dynamics simulation with the distance-dependent dielectric approximation. The time series illustrates the motion of Phe^{82} from its initial position in the heme crevice of cytochrome c to a bridging position between the hemes.

remainder of the simulation. Moreover, both the motions within the individual molecules and the relative motions between them in the complex are less pronounced than in the nonsolvated simulation (Fig. 2). For example, after 98 psec of simulation, the individual α-carbon backbones of cytochrome c and cytochrome b_5 change, respectively, by 1.2 and 1.3 Å rms, whereas cytochrome b_5 is displaced 4.4 Å rms from its initial position in the complex relative to cytochrome c. Although these displacements are smaller (on the time scale investigated by the simulation) than those found in the nonsolvated simulation, complex flexibility after equilibration is increased, as reflected by the relatively slow and large amplitude (±1.0 Å) variations in interheme iron distance (Fig. 2B). Collectively, these observations suggest that the inclusion of specific solvation attenuates electrostatic forces at the intermolecular interface relative to the nonsolvated simulation, which leads to less abrupt relaxation at the beginning of the simulation and more flexibility between reaction partners after equilibration.

Although the conformational change in Phe^{82} of cytochrome c evolved slightly differently from other early events in the nonsolvated simulation (Fig. 2A), its motion could have been due to coupling to the initial complex compression. However, motion of Phe^{82} in the solvated complex is uncoupled from initial relaxation events. About 98 psec of simulation are required for Phe^{82} to meander through its conformational change and eventually arrive at a heme-bridging orientation that is qualitatively similar to the abrupt shift seen in the nonsolvated simulation.

The molecular dynamics simulations illuminate several aspects of both the specific reaction of cytochromes c and b_5 and general reactions of reversibly bound electron transfer proteins.

1) The complementary electrostatic interactions that stabilize and orient the reaction partners in the complex are quite flexible. These associations thus differ from enzyme-substrate complexes or oligomeric proteins that typically incorporate specific packing interactions and directional hydrogen bonds to more rigidly fix intermolecular geometry. The interaction flexibility manifests itself in the relative lack of recognition specificity that is observed between electron transfer proteins. This allows many nonphysiological reaction partners, like cytochrome c and cytochrome b_5, to react as fast as genuine physiological partners, provided that appropriate surface charge distributions that are required for molecular orientation are preserved (*11*).

2) Molecular dynamics produce complex configurations that are substantially different from and potentially more favorable for electron transfer reactions than those obtained by computer graphics studies of the docking of static crystal structures. In both simulations, rearrangements at the protein interface produced inter-iron interaction distances that were 1.1 to 2.1 Å closer on average than the 17.8 Å distance in the corresponding static model. In addition, dynamic flexibility in the complex allows a range of interheme orientations and distances to be sampled over the lifetime of the complex. Although further studies are required to quantitatively evaluate the effects of such motions on electron transfer rates, both theoretical studies and experimental data suggest exponential dependencies of electron transfer rate on the distance between reacting prosthetic groups (*8, 16*).

3) Simulation of complex dynamics results in a relocation of the phenyl side chain of Phe^{82} in cytochrome c to a position where it bridges the cytochrome c and b_5 heme groups. The motion of Phe^{82} is facilitated by its location in a region of extended chain whose backbone peptide groups do not form α-helical or β-sheet secondary structures that could impede its flexibility (*17*). The major effect of complex formation on Phe^{82} motion appears to be the formation of an interface environment that traps Phe^{82} in a bridging conformation between the hemes. Although previous considerations of the role of aromatic side chains in cytochrome c have tended to rule against their participation as stable radical intermediates in electron transfer (*3, 4*), the simulated interaction could be functionally significant in coupling the heme electronic systems or displacing solvent trapped at the molecular interface or both (*4, 16*). In this context, recent experiments by Liang *et al.* (*18*) have demonstrated that substitution of the Phe^{82} homolog in yeast cytochrome c by tyrosine leaves intact its ability to transfer electrons to zinc-substituted cytochrome c peroxidase, whereas substitution by nonaromatic amino acids slows electron transfer by a factor of 10^4. These observations appear consistent with the inferred participation of Phe^{82}, a residue that is evolutionarily conserved among members of the cytochrome c family, in the electron transfer mechanism.

REFERENCES AND NOTES

1. R. Swanson *et al.*, *J. Biol. Chem.* **252**, 759 (1977).
2. F. R. Salemme, S. T. Freer, Ng. H. Xuong, R. A. Alden, J. Kraut, *ibid.* **248**, 3910 (1973).
3. F. R. Salemme, J. Kraut, M. D. Kamen, *ibid.*, p. 7701.
4. F. R. Salemme, *Annu. Rev. Biochem.* **46**, 299 (1977).
5. P. Strittmater and J. Ozols, *J. Biol. Chem.* **241**, 4787 (1966).
6. F. S. Mathews, M. Levine, P. Argos, *J. Mol. Biol.* **64**, 449 (1972).
7. F. R. Salemme, *ibid.* **102**, 563 (1976).
8. J. J. Hopfield, *Proc. Natl. Acad. Sci. U.S.A.* **71**, 3640 (1974).
9. M. W. Makinen, S. A. Schichman, S. C. Hill, H. B. Gray, *Science* **222**, 929 (1983); S. Ng, M. B. Smith, H. T. Smith, F. Millett, *Biochemistry* **16**, 4975 (1977); G. L. McLendon, J. R. Winkler, D. G. Nocera, M. R. Mauk, A. G. Mauk, H. B. Gray, *J. Am. Chem. Soc.* **107**, 739 (1985); L. S. Reid, M. R. Mauk, A. G. Mauk, *ibid.* **106**, 2182 (1984).
10. T. L. Poulos and B. C. Finzel, in *Peptide and Protein Reviews*, M. T. W. Hearn (Dekker, New York, 1984), vol. 4, p. 115; P. C. Weber and G. Tollin, *J. Biol. Chem.* **260**, 5568 (1985).
11. J. B. Matthew, P. C. Weber, F. R. Salemme, F. M. Richards, *Nature (London)* **301**, 169 (1983); M. R. Mauk, A. G. Mauk, P. C. Weber, J. B. Matthew, *Biochemistry* **25**, 7085 (1986).
12. F. C. Bernstein *et al.*, *J. Mol. Biol.* **112**, 535 (1977).
13. Initial model complex coordinates were energy minimized with the AMBER force field [P. Weiner and P. A. Kollman, *J. Comput. Chem.* **2**, 287 (1981); U. C. Singh and P. A. Kollman, *ibid.* **5**, 129 (1984); S. J. Weiner *et al.*, *J. Am. Chem. Soc.* **106**, 765 (1984)], and the united atom approximation until the root-mean-square change in the gradient was less than 0.01 Å. The molecular dynamics simulation was performed on a CRAY 1A computer with the AMBER force field and electrostatic forces scaled by a distance-dependent dielectric constant ($\epsilon = R_{ij}$), that included interactions from all atoms within a 9.5 Å nonbonded cutoff radius. The simulation, which incorporated 1908 atoms (including hydrogen atoms bound to polar protein groups), was initiated by applying a Maxwellian distribution of atomic velocities corresponding to a temperature of 300 K. The trajectory was computed in time increments of 0.001 psec, with coupling to a 300 K thermal bath [H. J. C. Berendsen, J. P. M. Postma, A. di Nola, W. F. van Gunsteren, J. R. Haak, *J. Chem. Phys.* **81**, 3684 (1984)] with a temperature relaxation constant of 0.1 psec. The lengths of covalent bonds to hydrogen were fixed during the simulation with the SHAKE algorithm [J. P. Ryckaert, G. Cicotti, H. J. C. Berendsen, *J. Comput. Phys.* **23**, 327 (1977); W. F. Van Gunsteren and H. J. C. Berendsen, *Mol. Phys.* **34**, 1311 (1977)].
14. J. B. Matthew and J. J. Wendoloski, *Biophys. J.* **51**, 404a (1987).
15. A 140-psec molecular dynamics simulation of the complex solvated with a 6 Å shell of 1222 TIP3P water molecules [W. L. Jorgensen, J. Chandrasekhar, J. Madura, R. W. Impey, M. L. Klein, *J. Chem. Phys.* **79**, 926 (1983)] was performed with an implementation of AMBER interfaced to GEMM, which is a molecular dynamics program implemented on the STAR Technologies ST-100 array processor [B. R. Brooks, in *Supercomputer Research in Chemistry and Chemical Engineering*, C. Jensen and D. Truhlar, Eds. (American Chemical Society, Washington, DC, in press)]. Since water was explicitly incorporated in the simulation, electrostatic interactions were computed with a constant dielectric of $\epsilon = 1$ and a 9.5 Å nonbonded interaction radius. The simulation was initiated by incrementing the atomic velocities in 30 K steps every 0.2 psec until the system reached 300 K and then allowing the system to equilibrate for an additional 23 psec. Trajectory integration for an additional 115 psec was performed with a 0.001-psec time increment.
16. R. A. Scott, A. G. Mauk, H. B. Gray, *J. Chem. Educ.* **62**, 932 (1985); R. A. Marcus, *Annu. Rev. Phys. Chem.* **15**, 155 (1964); S. Wherland and H. B. Gray, *Proc. Natl. Acad. Sci. U.S.A.* **73**, 2950 (1976); S. L. Mayo, W. R. Ellis, Jr., R. J. Crutchley, H. B. Gray, *Science* **233**, 948 (1986).
17. S. H. Northrup, M. R. Pear, J. D. Morgan, J. A. McCammon, M. Karplus, *J. Mol. Biol.* **153**, 1087 (1981), have described molecular dynamics simulations of cytochrome c that show chain flexibility in regions near Phe^{82}. Recent simulations show occasional fluctuations of Phe^{82} out of the heme crevice [see (*14*)].
18. N. Liang, G. J. Pielak, A. G. Mauk, M. Smith, B. M. Hoffman, *Proc. Natl. Acad. Sci. U.S.A.* **84**, 1249 (1987).
19. We thank B. Brooks for making available his GEMM STAR ST100 array processor code and

aiding in its installation, M. Levitt for numerous helpful and critical discussions, Z. Wasserman for important contributions to code development and methodology, and R. Hilmer for the interactive computer graphics used in the analysis of molecular dynamics simulations.

29 June 1987; accepted 1 September 1987

A Nerve Growth Factor–Induced Gene Encodes a Possible Transcriptional Regulatory Factor

JEFFREY MILBRANDT

Nerve growth factor (NGF) is a trophic agent that promotes the outgrowth of nerve fibers from sympathetic and sensory ganglia. The neuronal differentiation stimulated by this hormone was examined in the NGF-responsive cell line PC12. Differential hybridization was used to screen a complementary DNA library constructed from PC12 cells treated with NGF and cycloheximide. One of the complementary DNA clones that was rapidly induced by NGF was found to have a nucleotide sequence that predicts a 54-kilodalton protein with homology to transcriptional regulatory proteins. This clone, NGFI-A, contains three tandemly repeated copies of the 28– to 30–amino acid "zinc finger" domain present in *Xenopus laevis* TFIIIA and other DNA-binding proteins. It also contains another highly conserved unit of eight amino acids that is repeated at least 11 times. The NGFI-A gene is expressed at relatively high levels in the brain, lung, and superior cervical ganglion of the adult rat.

NERVE GROWTH FACTOR (NGF) IS a polypeptide hormone that is required for the development and survival of sympathetic and neural crest–derived sensory neurons in vivo and in vitro (*1*). NGF also participates in nerve regeneration after injury (*2*) and plays a role in the central nervous system (*3*). The effects of NGF on the differentiation of sympathetic neurons are manifested by an accelerated outgrowth of nerve fibers and the induction of several enzymes involved in neurotransmitter biosynthesis (*4*). During the differentiation process, specific genes are turned on and off at precise times. This ordered pattern of gene expression, resulting in the establishment of the neuronal phenotype, is presumably controlled by DNA-binding proteins that act to regulate transcription.

The best characterized transcriptional activating factor is the TFIIIA protein that regulates the expression of 5*S* RNA genes during development in *Xenopus laevis* (*5*). The DNA-binding region of this protein is composed of nine tandemly repeated units that contain two invariant pairs of Cys and His residues (*6*). Each repeat unit is folded around a single zinc ion that is coordinately bonded to the Cys and His residues to form a DNA-binding domain or "Zn finger." Amino acids capable of interacting with the DNA helix (Lys, His, Asn, Gln, Thr, and Arg) are located at the tip of each "Zn finger." This 28– to 30–amino acid DNA-binding domain has now been identified in several other proteins involved in transcriptional regulation, including yeast ADR1-encoded protein (*7*) and the Kruppel gene of *Drosophila* (*8*).

One model of neuronal differentiation is the PC12 cell line (*9*), whose NGF-mediated transition from replicating adrenal chromaffin-like cells to sympathetic neuron-like cells is prevented by the addition of RNA synthesis inhibitors (*10*). This cell line, derived from a rat pheochromocytoma, responds to NGF by extending neurites and by increasing the transcription of several genes, including ornithine decarboxylase (*11*), GAP43 (*12*), and c-*fos* (*13*). The activation of the proto-oncogene c-*fos* is rapid but transient in NGF-treated PC12 cells. The c-*fos* transcripts accumulate to even higher levels in cells stimulated in the presence of cycloheximide (CHX), in part because of an increase in messenger RNA (mRNA) half-life (*14*). Using c-*fos* as a model of an early activated gene, I have taken advantage of this CHX-mediated superinduction to identify other early, NGF-induced genes that may regulate neuronal differentiation.

A complementary DNA (cDNA) library containing 8×10^5 independent clones was constructed in the vector λgt10 (*15*), by using mRNA isolated from PC12 cells that had been treated with NGF (50 ng/ml) and CHX (10 μg/ml) for 3 hours. Initially, 8000 recombinants (1% of total library) were screened by differential hybridization with single-stranded cDNA probes complementary to mRNA from either unstimulated PC12 cells (no NGF) or PC12 cells treated with NGF and CHX for 3 hours. Three different NGF-induced cDNAs were identified from this screen: c-*fos*, a protein that binds DNA (*16*) and may function as a trans-acting factor (*17*), NGFI-A, and NGFI-B.

NGFI-A was selected for further study. This cDNA hybridized to a ~3.3-kb mRNA that was induced by NGF (Fig. 1A, lane 3) but accumulated to a much higher level in PC12 cells treated with NGF and CHX (lane 4). In PC12 cells grown without NGF this mRNA could not be detected (lane 1). However, when cells were treated with CHX alone, the level of this transcript was slightly increased (lane 2).

The time course of induction of the NGFI-A mRNA was determined by isolating mRNA from PC12 cells treated with NGF for various lengths of time. Northern analysis with the NGFI-A cDNA probe showed that the basal level of this transcript was very low in PC12 cells (Fig. 1B), but within 15 minutes after the addition of NGF (lane 2) the level of NGFI-A mRNA

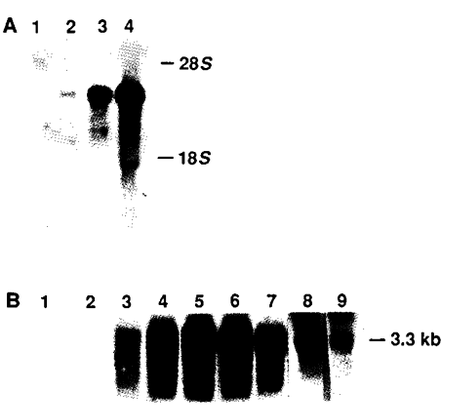

Fig. 1. Identification of an NGF-regulated cDNA clone. Total cellular RNA was isolated by the method of Chirgwin (*24*). The cDNA library was screened by differential hybridization with single-stranded cDNA probes complementary to mRNA from either naïve PC12 cells (no NGF) or PC12 cells treated with NGF and CHX for 3 hours (*25*). Phage from the NGFI-A cDNA clone were isolated on DEAE columns (*26*). DNA was purified and digested with Eco RI. The cDNA insert was isolated by electrophoresis on low-melting agarose and labeled with ^{32}P-labeled deoxyadenosine triphosphate by oligo labeling (*27*). RNA electrophoresis and Northern blot analysis were performed as described (*13*). (**A**) A Northern blot containing RNAs from PC12 cells treated for 3 hours with (lane 1) no addition, (lane 2) CHX (10 μg/ml), (lane 3) NGF (50 ng/ml), or (lane 4) NGF and CHX, was probed with the NGFI-A cDNA. The locations of the 28*S* and 18*S* ribosomal RNAs are indicated. (**B**) Time course of the NGF-mediated induction of NGFI-A mRNA. RNA samples from PC12 cells grown in the presence of NGF for 0, 2, 15, 30, 45, 60, and 120 minutes, 13 hours, and 6 days (lanes 1 through 9, respectively) were hybridized to ^{32}P-labeled NGFI-A cDNA insert. The 3.3-kb NGFI-A mRNA is indicated.

Division of Laboratory Medicine, Departments of Pathology and Internal Medicine, Washington University School of Medicine, St. Louis, MO 63110.